Supplemental Material: Emergence of X-states in a quantum impurity model

Moallison F. Cavalcante,[1,2,3,*] Marcus V. S. Bonança,[3] Eduardo Miranda,[3] and Sebastian Deffner[1,2,4]

[1] *Department of Physics, University of Maryland, Baltimore County, Baltimore, MD 21250, USA*
[2] *Quantum Science Institute, University of Maryland, Baltimore County, Baltimore, MD 21250, USA*
[3] *Gleb Wataghin Physics Institute, The University of Campinas, 13083-859, Campinas, São Paulo, Brazil*
[4] *National Quantum Laboratory, College Park, MD 20740, USA*

(Dated: April 10, 2025)

In this Supplementary Material, we provide details on (i) the impurity model, (ii) the OTOC calculations, (iii) the long-time behaviors of the correlation functions, (iv) the reduced density state for the localized edge modes, and (v) the information characterization of our X-state.

I. MODEL

The open boundary condition spin-1/2 chain with an edge-impurity is described by the Hamiltonian [1]

$$H_0 = -\sum_{j=1}^{N-1}\sigma_j^x\sigma_{j+1}^x - h\sum_{j=2}^{N}\sigma_j^z - h\mu\sigma_1^z, \tag{1}$$

where $\sigma_j^{a=x,y,z}$ are the Pauli matrices at the site j and μ defines the impurity at the edge. After applying the Jordan-Wigner transformation [2, 3], $\sigma_j^+ = (\sigma_j^x + i\sigma_j^y)/2 = (-1)^j \exp\left(i\pi\sum_{i=1}^{j-1} c_i^\dagger c_i\right) c_j^\dagger$ and $\sigma_j^z = 2c_j^\dagger c_j - 1$, the Hamiltonian of Eq. (1) reads

$$H_0 = \sum_{ij}\left[c_i^\dagger A_{ij} c_j + \frac{1}{2}\left(c_i^\dagger B_{ij} c_j^\dagger + \text{H.c.}\right)\right], \tag{2}$$

where $A_{ij} = 2h\left[(1-\mu)\delta_{i1} - 1\right]\delta_{ij} + (\delta_{i,j+1} + \delta_{i+1,j}) = A_{ji}$ and $B_{ij} = (\delta_{i+1,j} - \delta_{i,j+1}) = -B_{ji}$. Following [1, 2, 4, 5], the Hamiltonian (2) can be brought to the form

$$H_0 = \sum_\kappa \Gamma_\kappa \gamma_\kappa^\dagger \gamma_\kappa + \text{const.}, \tag{3}$$

where $c_j = \sum_\kappa u_{j\kappa}\gamma_\kappa + v_{j\kappa}\gamma_\kappa^\dagger$ represents the Bogoliubov transformation [2]. γ_κ are fermionic degrees of freedom: $\gamma_{1,2}$ for the localized modes, and γ_k for the delocalized ones. To guarantee the correct fermionic anticommutation relations, $\{\gamma_\kappa^\dagger, \gamma_{\kappa'}\} = \delta_{\kappa\kappa'}$ and $\{\gamma^\dagger, \gamma_{\kappa'}\} = 0$, the wave functions $u_{j\kappa}$ and $v_{j\kappa}$ need to satisfy (in matrix notation): $\mathbf{1} = uu^{\mathrm{T}} + vv^{\mathrm{T}}$ and $\mathbf{0} = uv^{\mathrm{T}} + vu^{\mathrm{T}}$, where $\mathbf{1}$ is the identity matrix, $\mathbf{0}$ is the null matrix, and T denotes the transpose operation. The inverse transformation reads $\gamma_\kappa = \sum_j u_{j\kappa}c_j + v_{j\kappa}c_j^\dagger$. In what follows, we will work with the quantities $\psi_{j\kappa} \equiv u_{j\kappa} - v_{j\kappa}$ and $\phi_{j\kappa} \equiv u_{j\kappa} + v_{j\kappa}$.

As discussed in the main text, the edge modes $\gamma_{\ell=1,2}$ only appear in specific regions of the (h,μ)-phase diagram (see Fig. 1(b) in the main text). For the γ_2 mode, these regions are: $|\mu| > \sqrt{1+1/h}$ for all $h > 0$ and $|\mu| < \sqrt{1-1/h}$ for $h > 1$. The energy and wave functions of this mode are,

$$\begin{aligned}
\Gamma^{(2)} &= 2|\mu|\sqrt{\frac{1+(\mu^2-1)h^2}{\mu^2-1}},\\
\psi_j^{(2)} &= \frac{(-1)^j h^{-j}\sqrt{(\mu^2-1)^2h^2-1}}{(\mu^2-1)^j},\\
\phi_j^{(2)} &= \frac{1}{\Gamma^{(2)}}\big[-2h\psi_j^{(2)} + 2h(1-\mu)\delta_{j1}\psi_1^{(2)}\\
&\quad +2(1-\delta_{j1})\psi_{j-1}^{(2)}\big],
\end{aligned} \tag{4}$$

where, hereafter, we use the superscript (ℓ) to label the mode $\ell = 1, 2$. The γ_1 mode exists in the entire region $h < 1$ (topological phase of the Kitaev chain [6]). For this mode, we have

$$\begin{aligned}
\Gamma^{(1)} &\simeq \frac{2|\mu|(1-h^2)h^N}{\sqrt{|1+h^2(\mu^2-1)|}},\\
\psi_j^{(1)} &= \sqrt{1-h^2}h^N\left(h^{-j} - \frac{\mu^2 h^j}{1+h^2(\mu^2-1)}\right),\\
\phi_j^{(1)} &= -\frac{\text{sgn}(\mu)\sqrt{1-h^2}\sqrt{|1+h^2(\mu^2-1)|}}{h[1+h^2(\mu^2-1)]}\\
&\quad \times\left[\delta_{j1}(1-\mu)+\mu\right]h^j.
\end{aligned} \tag{5}$$

where $\text{sgn}\{\cdot\}$ is the sign function. Notice that in the limit $N\to\infty$, $\Gamma^{(1)}, \psi_1^{(1)} \to 0$.

Finally, for the delocalized modes γ_k, we have

$$\begin{aligned}
\Gamma_k &= 2\sqrt{1+h^2-2h\cos k},\\
\psi_{jk} &= \sqrt{\frac{2}{N}}\frac{\sin jk + h(\mu^2-1)\sin(j-1)k}{\sqrt{1+h^2(\mu^2-1)^2+2h(\mu^2-1)\cos k}},\\
\phi_{jk} &= \frac{1}{\Gamma_k}\big[-2h\psi_{jk} + 2h(1-\mu)\psi_{1k}\delta_{j1}\\
&\quad +2(1-\delta_{j1})\psi_{j-1,k}\big].
\end{aligned} \tag{6}$$

In the continuum limit, we can take $k \in [0,\pi]$ as usual [1]. We see that the system gap closes at $h = 1$, independently of μ, where the system undergoes a quantum phase transition [3].

* moallison@umbc.edu

Region	$\Phi(Jt \gg 1, \mu)$	$\mathcal{C}(Jt \gg 1, \mu)$
$h > 1$ and $\mu \lessgtr \sqrt{1 \mp 1/h}$	$t^{-3/2}$	Eq. (9)
$h > 1$ and $\mu = \sqrt{1 \mp 1/h}$	t^{-2}	t^{-1}
$h > 1$ and $\sqrt{1-1/h} < \mu < \sqrt{1+1/h}$	t^{-3}	t^{-3}
$h < 1$ and $\mu < \sqrt{1+1/h}$	$t^{-3/2}$	$\frac{2(1-h^2)^2}{[1+h^2(\mu^2-1)]^2} + \mathcal{O}(t^{-3/2})$
$h < 1$ and $\mu = \sqrt{1+1/h}$	$t^{-1/2}$	$2(1-h)^2 + \mathcal{O}(t^{-1/2})$
$h < 1$ and $\mu > \sqrt{1+1/h}$	Eq. (6)	$\propto 1 - (\text{const.}') \cos \Gamma^{(2)} t$

TABLE I. Asymptotic behaviors of the response function, Eq. (4), and the OTOC, Eq. (7), for the different boundary phases of the model in Eq. (1).

A. Majorana representation

The model of Eq. (1) can be rewritten in terms of Majorana fermions. As discussed in the main text, this representation is useful for the calculation of the OTOC.

Decomposing the spinless fermionic operators c_i in the basis, $c_j^\dagger = \frac{a_j - i b_j}{2}$ and $c_j = \frac{a_j + i b_j}{2}$, where a_j and b_j are Majorana fermions, $a_j^2 = b_j^2 = 1$, $\{a_j, a_{j'}\} = \{b_j, b_{j'}\} = 2\delta_{jj'}$ and $\{a_j, b_{j'}\} = 0$, the Hamiltonian of Eq. (2) is recast as

$$H_0 = ih\mu b_1 a_1 + ih \sum_{j=2}^{N} b_j a_j - i \sum_{j=1}^{N-1} b_j a_{j+1} + \text{const.}. \quad (7)$$

In particular, when $\mu = 0$, we can see that the Majorana fermion a_1 totally decouples from the rest of the chain, $[a_1, H_0] = 0$, and thus it becomes a Majorana zero mode.

Another Majorana representation for the model (1) can be obtained by defining the new real fermions as follows: $\eta_{A,j} = i(c_j^\dagger - c_j)$ and $\eta_{B,j-1} = (c_j^\dagger + c_j)$, where $\eta_{A,j}^2 = \eta_{B,j}^2 = 1$, $\{\eta_{A,j}, \eta_{A,j'}\} = \{\eta_{B,j}, \eta_{B,j'}\} = 2\delta_{jj'}$ and $\{\eta_{A,j}, \eta_{B,j'}\} = 0$. Using this new basis, the Hamiltonian (1) reads now

$$h^{-1} H_0 = -i\mu \eta_{B,0} \eta_{A,1} - i \sum_{j=1}^{N-1} \eta_{B,j} \eta_{A,j+1} - ih^{-1} \sum_{j=1}^{N} \eta_{A,j} \eta_{B,j}, \quad (8)$$

where the const. term was ignored. The right-hand side of the above equation is exactly the Hamiltonian considered in [7] (see its Eq. (4)) once we make $h^{-1} \to h$ and identify $\eta_{B,0}$ as the ancilla Majorana fermion defined there.

II. OTOC CALCULATION

Here, we are interested in the OTOC,

$$\begin{aligned} \mathcal{C}(t,\mu) &= \frac{1}{2} \langle |[\sigma_1^z(t), \sigma_1^z(0)]|^2 \rangle_0, \\ &= 1 - \text{Re}\{F(t,\mu)\}, \end{aligned} \quad (9)$$

where $F(t,\mu) = \langle \sigma_1^z(t)\sigma_1^z(0)\sigma_1^z(t)\sigma_1^z(0) \rangle_0$ and $\text{Re}\{\cdots\}$ denotes the real part. Using the first Majorana representation discussed earlier, we can rewrite $\sigma_1^z = i a_1 b_1$ so that

$$F(t,\mu) = \langle a_1(t) b_1(t) a_1 b_1 a_1(t) b_1(t) a_1 b_1 \rangle_0. \quad (10)$$

The above OTOC can be calculated applying Wick's theorem since a_1 and b_1 are linear combinations of γ_κ and $\gamma_\kappa^\dagger$. However, as shown in reference [8], this expectation value can be cast in the form of a Pfaffian of a matrix $\mathcal{M}(t)$,

$$F(t,\mu) = \text{Pf}\{\mathcal{M}(t)\}. \quad (11)$$

For our case,

$$\mathcal{M}(t) = \begin{pmatrix} \mathcal{A}(0) & \mathcal{B}(t) & \mathbf{1} + \mathcal{A}(0) & \mathcal{B}(t) \\ -\mathcal{B}^{\mathrm{T}}(t) & \mathcal{A}(0) & \mathcal{B}(-t) & \mathbf{1} + \mathcal{A}(0) \\ -\mathbf{1} + \mathcal{A}(0) & -\mathcal{B}^{\mathrm{T}}(-t) & \mathcal{A}(0) & \mathcal{B}(t) \\ -\mathcal{B}^{\mathrm{T}}(t) & -\mathbf{1} + \mathcal{A}(0) & -\mathcal{B}^{\mathrm{T}}(t) & \mathcal{A}(0) \end{pmatrix}, \quad (12)$$

where we defined the 2×2 matrices

$$\mathcal{A}(t) = \begin{pmatrix} 0 & G_{ab}(t) \\ -G_{ab}(t) & 0 \end{pmatrix}, \quad (13)$$

$$\mathcal{B}(t) = \begin{pmatrix} G_{aa}(t) & G_{ab}(t) \\ G_{ba}(t) & G_{bb}(t) \end{pmatrix}. \quad (14)$$

Here, $G_{rr'}(t) \equiv \langle r(t) r'(0) \rangle_0$, where $r, r' = a_1, b_1$, and $\mathbf{1}$ is the 2×2 identity matrix. Notice that $\mathcal{A}(t) = -\mathcal{A}^{\mathrm{T}}(t)$.

Since, like the determinant, the Pfaffian is invariant under the addition of rows and columns, we obtain

$$F(t,\mu) = \text{Pf}\{\tilde{\mathcal{M}}(t)\}, \quad (15)$$

where

$$\tilde{\mathcal{M}}(t) = \begin{pmatrix} \mathcal{A}(0) & \mathcal{B}(t) & \mathbf{1} & \mathbf{0} \\ -\mathcal{B}^{\mathrm{T}}(t) & \mathcal{A}(0) & \mathbf{0} & \mathbf{1} \\ -\mathbf{1} & \mathbf{0} & \mathbf{0} & \mathcal{B}(t) + \mathcal{B}^{\mathrm{T}}(-t) \\ \mathbf{0} & -\mathbf{1} & -\mathcal{B}^{\mathrm{T}}(t) - \mathcal{B}(-t) & \mathbf{0} \end{pmatrix}, \quad (16)$$

and $\mathbf{0}$ is the 2×2 null matrix. Performing the calculation, we find [8]

$$
\begin{aligned}
2^{-1}\mathcal{C}(t,\mu) = &(\mathrm{Re}\{G_{ba}(t)\})^2 + (\mathrm{Re}\{G_{ab}(t)\})^2 + (\mathrm{Re}\{G_{aa}(t)\})^2 + (\mathrm{Re}\{G_{bb}(t)\})^2 \\
&-2\Big[\mathrm{Re}\{G_{ba}(t)\}\mathrm{Re}\{G_{ab}(t)\} - \mathrm{Re}\{G_{aa}(t)\}\mathrm{Re}\{G_{bb}(t)\}\Big]\Big[\mathrm{Re}\{G^2_{ab}(0)\} \\
&+\mathrm{Re}\{G_{ab}(t)\}\mathrm{Re}\{G_{ba}(t)\} - \mathrm{Im}\{G_{ab}(t)\}\mathrm{Im}\{G_{ba}(t)\} \\
&-\mathrm{Re}\{G_{aa}(t)\}\mathrm{Re}\{G_{bb}(t)\} + \mathrm{Im}\{G_{aa}(t)\}\mathrm{Im}\{G_{bb}(t)\}\Big],
\end{aligned} \tag{17}
$$

where $\mathrm{Im}\{\cdot\}$ denotes the imaginary part.

The two-point Majorana correlation functions in the above expression, $G_{rr'}(t)$, are given by

$$
\begin{aligned}
G_{ab}(t) &= i\sum_\kappa \phi_\kappa \psi_\kappa e^{-i\Gamma_\kappa t}, \\
G_{ba}(t) &= [G_{ab}(-t)]^*, \\
G_{aa}(t) &= \sum_\kappa \phi_\kappa^2 e^{-i\Gamma_\kappa t}, \\
G_{bb}(t) &= \sum_\kappa \psi_\kappa^2 e^{-i\Gamma_\kappa t},
\end{aligned} \tag{18}
$$

where the above summations include both the delocalized and the localized modes, and we used the notation $\psi_{1\kappa} \equiv \psi_\kappa$.

III. STATIONARY PHASE APPROXIMATION (SPA)

The long-time power-law behaviors observed for the response function and the OTOC (see Figs. 2 and 3 in the main text) can be understood by applying the stationary phase approximation (SPA) [9].

A. Response function $\Phi(t,\mu)$

In the limit $N \to \infty$, the summation over the bulk modes in Eq. (5) is converted to an integral. In the red region of Fig. 1(b), where we only have delocalized modes, the response function is given by

$$
\Phi(t,\mu) = \int_0^\pi dk dk' f_{kk'} \sin[(\Gamma_k + \Gamma_{k'})t]. \tag{19}
$$

The long-time limit ($t \gg J^{-1}$) of $\Phi(t,\mu)$ is obtained by performing the integration of $f_{kk'}\sin[(\Gamma_k + \Gamma_{k'})t]$ expanded near the extreme points of $\Gamma_k + \Gamma_{k'}$: $\{(0,0),(0,\pi),(\pi,0),(\pi,\pi)\}$ [see Eq. (6)]. Expanding around the points $\{(0,0),(\pi,\pi)\}$ gives us $f_{kk'} \sim k^2 k'^2 (k^2 - k'^2)$, which produces a decay faster than t^{-3}. If we expand $f_{kk'}$ around $(0,\pi)$ (or, equivalently, around $(\pi,0)$), we obtain $f_{kk'} \sim k^2 (k' - \pi)^2$. This leads to, $\Phi(t \gg J^{-1},\mu) \sim \left(t^{-3/2}\right)^2 = t^{-3}$, which agrees with the numerical calculation of Eq. (5), see Fig. 2(a, b) in the main text.

When only one of the localized modes $\gamma_{\ell=1,2}$ is present (and far from the boundaries), besides the contribution in Eq. (19), we also have the term $\int_0^\pi dk\ (f_{k\ell} + f_{\ell k})\sin[(\Gamma_k + \Gamma^{(\ell)})t]$. For the latter, obviously, the extreme points are $k = 0, \pi$, and both of them give the same result, $f_{k\ell} \sim k^2$ (when expanded around $k = \pi$, we have done a π-translation). Thus, $\Phi(t \gg J^{-1},\mu) \sim t^{-3/2}$. At the boundaries, $h > 1$ and $\mu = \sqrt{1 \mp 1/h}$, $f_{kk'}$ behaves as $f_{kk'} \sim k^2$ around $(0,\pi)$. Then, $\Phi(t \gg J^{-1},\mu) \sim t^{-3/2} t^{-1/2} = t^{-2}$. However, at the boundary $\mu = \sqrt{1 + 1/h}$ and $h < 1$, the mode γ_1 contributes, making $f_{k,\ell=1} \sim 1$ around $k = \pi$. This produces the slower decay seen in Fig. 2(c), $\Phi(t \gg J^{-1},\mu) \sim t^{-1/2}$.

B. OTOC $\mathcal{C}(t,\mu)$

As we saw in the Sec. II, to calculate $\mathcal{C}(t,\mu)$ we need to know the two-point Majorana correlation functions, $G_{rr'}(t)$, see Eq. (17). The long-time behavior of $G_{rr'}(t)$ can be extracted from the SPA discussed above. In the red region of Fig. 1(b) (only delocalized modes), from Eq. (6) we obtain $\psi_k, \phi_k \sim k$ around $k = 0$. Thus, $G_{rr'}(t \gg J^{-1}) \sim t^{-3/2}$ (see Eq. (18)). This leads to $\mathcal{C}(t \gg J^{-1},\mu) \sim t^{-3}$. At the boundaries $h > 1$ and $\mu = \sqrt{1 \mp 1/h}$, $\psi_k, \phi_k \sim 1$ (for $\mu = \sqrt{1 - 1/h}$ we have expanded around $k = 0$ while for $\mu = \sqrt{1 + 1/h}$ around $k = \pi$). Then, $G_{rr'}(t \gg J^{-1}) \sim t^{-1/2}$, which produces $\mathcal{C}(t \gg J^{-1},\mu) \sim t^{-1}$.

In table I we summarize all the results for the asymptotic behaviors of $\Phi(t,\mu)$ and $\mathcal{C}(t,\mu)$.

IV. REDUCED STATE FOR THE LOCALIZED MODES

For the system initially prepared in its ground state $|\mathbf{0}\rangle$ within the yellow region of Fig. 1(b) (where both $\gamma_{1,2}$ edge modes are present), we turn on the impulsive perturbation $-g_0\delta(t)\sigma_1^z$. The system state at time $t > 0$ will be given by

$$
|\Psi(t)\rangle = e^{-iH_0 t} T \exp\left[-i\int_0^t dt' \delta H(t')\right]|\mathbf{0}\rangle, \tag{20}
$$

where $\delta H(t) = -g_0\delta(t)\sigma_1^z(t)$, with $\sigma_1^z(t) = e^{iH_0 t}\sigma_1^z e^{-iH_0 t}$, and T is the time ordering operator. Using the Dirac delta function property,

$$
|\Psi(t)\rangle = \left(\cos g_0 \mathbf{1} + i \sin g_0 e^{-iH_0 t}\sigma_1^z\right)|\mathbf{0}\rangle, \tag{21}
$$

where it was considered that $H_0|\mathbf{0}\rangle = 0$. Thus, the system density operator reads,

$$\begin{aligned}\rho(t) &= |\Psi(t)\rangle\langle\Psi(t)|,\\ &= \cos^2 g_0\,(|\mathbf{0}\rangle\langle\mathbf{0}|) - i\frac{\sin 2g_0}{2}\left(|\mathbf{0}\rangle\langle\mathbf{0}|\sigma_1^z e^{iH_0t}\right),\\ &\quad + i\frac{\sin 2g_0}{2}\left(e^{-iH_0t}\sigma_1^z|\mathbf{0}\rangle\langle\mathbf{0}|\right),\\ &\quad + \sin^2 g_0\left(e^{-iH_0t}\sigma_1^z|\mathbf{0}\rangle\langle\mathbf{0}|\sigma_1^z e^{iH_0t}\right). \end{aligned} \tag{22}$$

The density operator $\rho(t)$, being the state of the full system, provides the time evolution of any average value, in particular, the local magnetization of the impurity, given by $\langle\sigma_1^z(t)\rangle$. However, $\langle\sigma_1^z(t)\rangle$ can also be obtained from the response function (4) in the perturbative regime and, as shown in Fig.2(c) of the main text, its long-time behavior has persistent oscillations when the two localized modes are present. Next, we show that this is a signature of the X-state in the reduced density operator of the localized modes and that couplings (in the sense of non-diagonal matrix elements of $\rho(t)$) introduced by the perturbation between the edge and bulk modes with different number of excitations in the later ones decay in the long-time limit. To see this, we express $\langle\sigma_1^z(t)\rangle$ as follows,

$$\begin{aligned}\langle\sigma_1^z(t)\rangle &= \mathrm{Tr}\{\rho(t)\sigma_1^z\},\\ &= \sum_{n,n'}\langle n|\rho(t)|n'\rangle\langle n'|\sigma_1^z|n\rangle, \end{aligned} \tag{23}$$

where $|n\rangle$ and $|n'\rangle$ are two Fock states: $|n\rangle \equiv |n_1, n_2\rangle \otimes |\nu_1, \nu_2, \cdots\rangle$, being $|n_1, n_2\rangle$ (with $n_{\ell=1,2} = 0, 1$) the localized edge modes part and $|\nu_1, \nu_2, \cdots\rangle$ (with $\nu_i = 0, 1$) the delocalized modes part. Because σ_1^z creates zero or two γ_κ excitations ($\sigma_j^z = 2c_j^\dagger c_j - 1$), the non-zero terms in the above expression are terms where $|n\rangle$ and $|n'\rangle$ differ by zero or two excitations. These excitations can occupy edge or bulk modes. However, in the long-time limit, $t \gg J^{-1}$, not all of those terms will survive due to the presence of high oscillatory factors. For instance, let us analyze the matrix elements $\langle kk'| \otimes \langle 0,0|\rho(t)|1,0\rangle \otimes |k''\rangle$, where $|k\rangle = \gamma_k^\dagger|0_d\rangle$ and $|kk'\rangle = \gamma_k^\dagger\gamma_{k'}^\dagger|0_d\rangle$, being $|0_d\rangle$ the delocalized fermionic vacuum, $\nu_i = 0$. The last term of Eq. (22) gives us (the others are zero),

$$\langle kk'| \otimes \langle 0,0|\rho(t)|1,0\rangle \otimes |k''\rangle \sim e^{-i(\Gamma_k+\Gamma_{k'}-\Gamma_{k''})t}. \tag{24}$$

Thus, the sum over all states like this in Eq. (23), is a sum of high oscillatory terms, which goes to zero when $t \gg J^{-1}$. Therefore, the only surviving coherences in the long-time limit are those corresponding to Fock states with equal number of excitations in the bulk modes. In the long-time limit, the relevant content of $\rho(t)$ is hence concentrated in the subspace spanned by the states with 0, 1 and 2 excitations in the edge modes, i.e., in the reduced density operator obtained by

$$\begin{aligned}\rho_{\mathrm{loc}}(t) &= \mathrm{Tr}_{\mathrm{del}}\,\rho(t),\\ &= \sum_{\nu_1,\nu_2,\cdots}\langle\nu_1,\nu_2,\cdots|\rho(t)|\nu_1,\nu_2,\cdots\rangle. \end{aligned} \tag{25}$$

After performing the above calculation, we find

$$\begin{aligned}\rho_{\mathrm{loc}}(t) = \rho_{11}|0,0\rangle\langle 0,0| + \rho_{22}|0,1\rangle\langle 0,1| + \rho_{33}|1,0\rangle\langle 1,0| + \rho_{44}|1,1\rangle\langle 1,1|,\\ +\rho_{14}(t)|0,0\rangle\langle 1,1| + \rho_{14}^*(t)|1,1\rangle\langle 0,0| + \rho_{23}^*(t)|1,0\rangle\langle 0,1| + \rho_{23}(t)|0,1\rangle\langle 1,0|. \end{aligned} \tag{26}$$

In the matrix representation this reads,

$$\rho_{\mathrm{loc}}(t) = \begin{pmatrix} \rho_{11} & 0 & 0 & \rho_{14}(t)\\ 0 & \rho_{22} & \rho_{23}(t) & 0\\ 0 & \rho_{23}^*(t) & \rho_{33} & 0\\ \rho_{14}^*(t) & 0 & 0 & \rho_{44}\end{pmatrix}, \tag{27}$$

where

$$\begin{aligned}\rho_{11} &= \cos^2 g_0 + \sin^2 g_0\left(|\Upsilon_1|^2 + \sum_{kk'(k\neq k)}|\Upsilon_2(k,k')|^2\right),\\ \rho_{22} &= \sin^2 g_0\sum_k|\Upsilon_3(k)|^2,\\ \rho_{33} &= \sin^2 g_0\sum_k|\Upsilon_4(k)|^2,\\ \rho_{44} &= \sin^2 g_0|\Upsilon_5|^2,\\ \rho_{14}(t) &= \Upsilon_5^*\left(\Upsilon_1\sin^2 g_0 - i\frac{\sin 2g_0}{2}\right),\\ \rho_{23}(t) &= \sin^2 g_0\sum_k\Upsilon_3(k)\Upsilon_4^*(k). \end{aligned} \tag{28}$$

The functions Υ_i in the above expressions are

$$\Upsilon_1 = -1 + 2\sum_k v_k^2, \tag{29}$$

$$\Upsilon_2(k,k') = 2e^{-i(\Gamma_k+\Gamma_{k'})t} v_{k'} u_k, \tag{30}$$

$$\Upsilon_3(k) = 2e^{-i(\Gamma_k+\Gamma^{(2)})t}\left[v^{(2)}u_k - v_k u^{(2)}\right], \tag{31}$$

$$\Upsilon_4(k) = 2e^{-i(\Gamma_k+\Gamma^{(1)})t}\left[v^{(1)}u_k - v_k u^{(1)}\right], \tag{32}$$

$$\Upsilon_5 = 2e^{-i(\Gamma^{(2)}+\Gamma^{(1)})t}\left[v^{(2)}u^{(1)} - v^{(1)}u^{(2)}\right]. \tag{33}$$

Notice that Υ_1 is time-independent.

V. PURITY, ENTANGLEMENT AND DISCORD

The purity is obtained as usual from $\mathrm{Tr}_{\rm loc}\rho_{\rm loc}^2(t)$, with $\rho_{\rm loc}(t)$ given by Eq. (10). The entanglement measure is given by the concurrence, $0 < C(\rho_{\rm loc}(t)) < 1$, which can be obtained in terms of the matrix elements of the X-state as follows [10]

$$C(\rho_{\rm loc}(t)) = \max\{0, 2(|\rho_{14}(t)| - \sqrt{\rho_{22}\rho_{33}}), 2(|\rho_{23}(t)| - \sqrt{\rho_{11}\rho_{44}})\}. \tag{34}$$

Finally, the discord is obtained following Refs. [11, 12]. In Figs. 1 and 2 we show the results for these three quantities assuming different h values.

[1] G. Francica, T. J. G. Apollaro, N. Lo Gullo, and F. Plastina, Local quench, majorana zero modes, and disturbance propagation in the ising chain, Phys. Rev. B **94**, 245103 (2016).

[2] E. Lieb, T. Schultz, and D. Mattis, Two soluble models of an antiferromagnetic chain, Annals of Physics **16**, 407 (1961).

[3] S. Sachdev, *Quantum Phase Transitions* (Cambridge University Press, Cambridge, 1999).

[4] L. Losonczi, Eigenvalues and eigenvectors of some tridiagonal matrices, Acta Mathematica Hungarica **60**, 309 (1992).

[5] W.-C. Yueh, Eigenvalues of several tridiagonal matrices, Appl. Math. E-Notes **5**, 66 (2005).

[6] A. Y. Kitaev, Unpaired majorana fermions in quantum wires, Physics-Uspekhi **44**, 131 (2001).

[7] U. Javed, J. Marino, V. Oganesyan, and M. Kolodrubetz, Counting edge modes via dynamics of boundary spin impurities, Phys. Rev. B **108**, L140301 (2023).

[8] C.-J. Lin and O. I. Motrunich, Out-of-time-ordered correlators in a quantum ising chain, Phys. Rev. B **97**, 144304 (2018).

[9] Y.-H. Huang, Y.-T. Zou, and C. Ding, Dynamical relaxation of a long-range kitaev chain, Phys. Rev. B **109**, 094309 (2024).

[10] T. Yu and J. Eberly, Sudden death of entanglement: Classical noise effects, Optics Communications **264**, 393 (2006).

[11] M. Ali, A. R. P. Rau, and G. Alber, Quantum discord for two-qubit x states, Phys. Rev. A **81**, 042105 (2010).

[12] Y. Huang, Quantum discord for two-qubit x states: Analytical formula with very small worst-case error, Phys. Rev. A **88**, 014302 (2013).

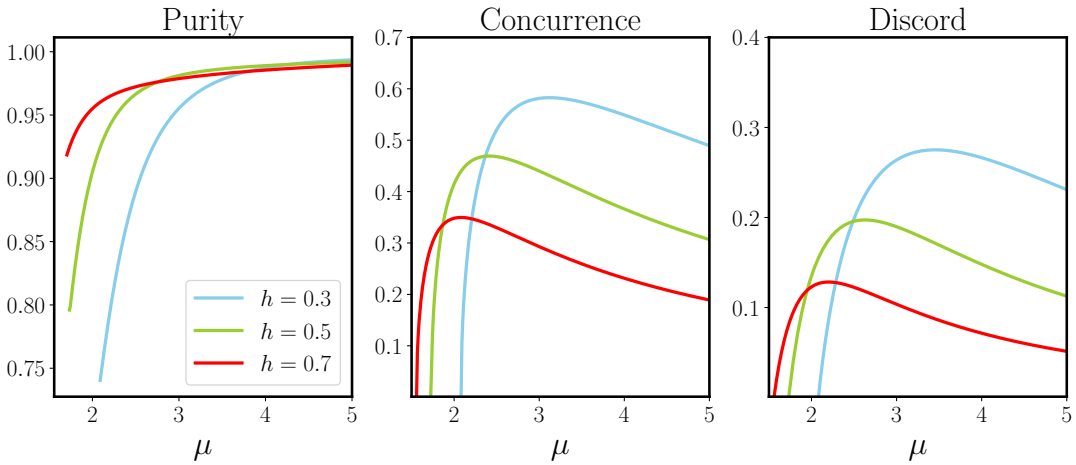

FIG. 1. Purity, concurrence and discord for the X-state in Eq. (9). The lower μ cutoffs of the purity curves come from the need to satisfy $\mu > \sqrt{1 + 1/h}$. Here we take $g_0 = 0.5$.

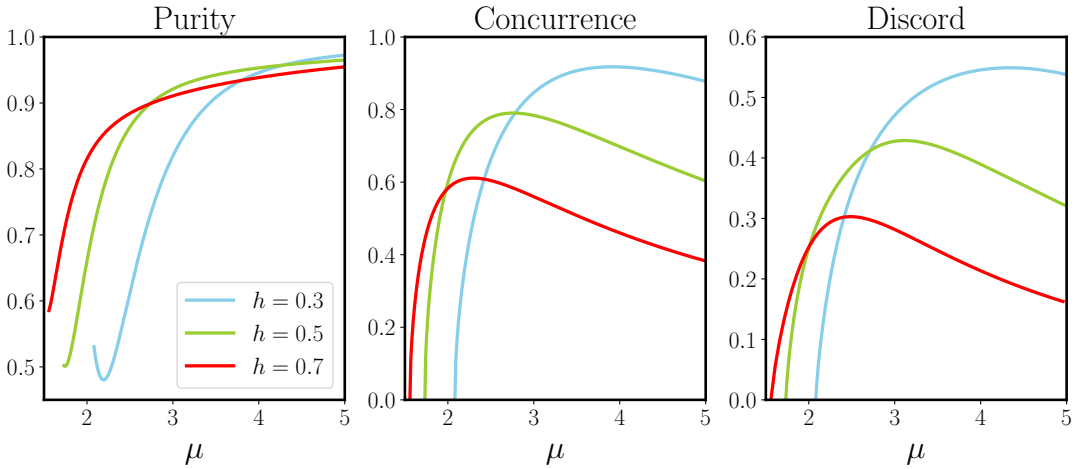

FIG. 2. Purity, concurrence and discord for the X-state in Eq. (9). The lower μ cutoffs of the purity curves come from the need to satisfy $\mu > \sqrt{1 + 1/h}$. Here we take $g_0 = \pi/2$.